THE JOURNAL OF BIOLOGICAL CHEMISTRY
Vol. 274, No. 19, Issue of May 7, pp. 13292–13297, 1999

Printed in U.S.A.

Site-directed Mutagenesis of Cytochrome c_6 from *Synechocystis* sp. PCC 6803

THE HEME PROTEIN POSSESSES A NEGATIVELY CHARGED AREA THAT MAY BE ISOFUNCTIONAL WITH THE ACIDIC PATCH OF PLASTOCYANIN*

(Received for publication, December 14, 1998, and in revised form, January 28, 1999)

Berta De la Cerda, Antonio Díaz-Quintana, José A. Navarro, Manuel Hervás, and Miguel A. De la Rosa‡

From the Instituto de Bioquímica Vegetal y Fotosíntesis, Universidad de Sevilla y CSIC, Centro Isla de la Cartuja, Américo Vespucio s/n, 41092 Sevilla, Spain

This paper reports the first site-directed mutagenesis analysis of any cytochrome c_6, a heme protein that performs the same function as the copper-protein plastocyanin in the electron transport chain of photosynthetic organisms. Photosystem I reduction by the mutants of cytochrome c_6 from the cyanobacterium *Synechocystis* sp. PCC 6803 has been studied by laser flash absorption spectroscopy. Their kinetic efficiency and thermodynamic properties have been compared with those of plastocyanin mutants from the same organism. Such a comparative study reveals that aspartates at positions 70 and 72 in cytochrome c_6 are located in an acidic patch that may be isofunctional with the well known "southeast" patch of plastocyanin. Calculations of surface electrostatic potential distribution in the mutants of cytochrome c_6 and plastocyanin indicate that the changes in protein reactivity depend on the surface electrostatic potential pattern rather than on the net charge modification induced by mutagenesis. Phe-64, which is close to the heme group and may be the counterpart of Tyr-83 in plastocyanin, does not appear to be involved in the electron transfer to photosystem I. In contrast, Arg-67, which is at the edge of the cytochrome c_6 acidic area, seems to be crucial for the interaction with the reaction center.

Cytochrome c_6 (Cyt)[1] and plastocyanin (Pc) are soluble metalloproteins, located inside the thylakoid lumen of photosynthetic organisms, that carry electrons from cytochrome b_6f to photosystem I (PSI), which are both membrane-anchored complexes. Although cyanobacteria and eukaryotic green alga can synthesize both Pc and Cyt, Pc seems to have been able to replace the primitive Cyt along evolution of photosynthetic organisms as the copper-protein is the only electron carrier in higher plants. The two metalloproteins are now well characterized, both at the structural and functional levels. Their three-dimensional structures have been solved by x-ray crystallography and NMR spectroscopy in several organisms, and their reaction mechanisms have been widely investigated (see Ref. 1 for a recent review).

Alignment of eukaryotic Pc and Cyt molecules according to their dipole moment and surface charge distribution has allowed us the observation of areas in the heme protein similar to those previously reported in Pc: i) a hydrophobic region around the surface-exposed heme edge that could be equivalent to the north patch involving the copper ligand His-87 in Pc, and ii) a negatively charged area in Cyt similar to the east acidic patch around Tyr-83 in Pc (1, 2). It should be noted that such an acidic patch is significantly smaller in the metalloproteins isolated from prokaryotes, namely the cyanobacterium *Synechocystis* sp. PCC 6803 in which the acidic patch is rather south-east-facing, just below Tyr-87.

In eukaryotic systems, site-directed mutagenesis of Pc has supplied relevant information on the role of specific residues in site 1 (or the hydrophobic north pole) and site 2 (or the acidic east face), which both have been proposed to be involved in the interaction with PSI (3–6). Whereas negative residues in the east face seem to be responsible for electrostatic interactions and complex formation with the positively charged PsaF subunit of PSI, the transfer of electrons from the Pc copper center to the chlorophyll dimer $P700^+$ in PSI could take place via the imidazole ring of His-87 (one of the four ligands to the copper atom) in the north pole.

In *Synechocystis*, in which wild type (WT) Cyt and Pc interact with PSI according to a simple oriented collisional reaction mechanism (7), we have recently carried out a functional site-directed mutagenesis analysis of Pc (8). This study showed that most of the mutants react following the same model as the WT protein, with the only exception of the double mutant D44R/D47R which is able to form a kinetically detectable electrostatic complex with PSI at low ionic strength, as do the eukaryotic copper proteins (9, 10). These findings indicate that the reaction mechanism of PSI reduction can be drastically modified by changing specific surface amino acids, mainly the acidic residues in the east face of the protein (8).

This paper describes the kinetic and thermodynamic properties of a set of mutants of *Synechocystis* Cyt, which has been modified in two specific residues located in a region equivalent to the east face of Pc, as well as in two others close to the heme

* This work was supported by the Dirección General de Investigación Científica y Técnica (DGICYT, Grant PB96-1381), European Union (EU, CHRX-CT94-0540 and ERB-FMRX-CT98-0218), and Junta de Andalucía (PAI, CVI-0198). The costs of publication of this article were defrayed in part by the payment of page charges. This article must therefore be hereby marked "*advertisement*" in accordance with 18 U.S.C. Section 1734 solely to indicate this fact.

‡ To whom correspondence should be addressed. Tel.: +34 954 489506; Fax: +34 954 460065; E-mail: marosa@cica.es.

[1] The abbreviations used are: Cyt, cytochrome c_6; k_{bim}, bimolecular rate constant for the overall reaction; k_{obs}, observed pseudo first-order rate constant; k_{∞}, diffusion-limited rate constant; Pc, plastocyanin; PSI, photosystem I; $\Delta G^{\neq}$, $\Delta H^{\neq}$, and $\Delta S^{\neq}$, activation free energy, enthalpy, and entropy of the overall reaction; $\Delta\Delta G^{\neq}$, change in the activation free energy of PSI reduction by mutant proteins as compared with that with the wild-type molecule; Δq, net charge difference between wild-type and mutant metalloproteins; V_{el}, difference in electrostatic energy between the wild-type and mutant proteins; V_{ii}, net electrostatic potential for the redox interaction; WT, wild-type; X_k, Debye-Hückel term accounting for charge screening; Tricine, *N*-[2-hydroxy-1,1-bis(hydroxymethyl)-ethyl]glycine; MES, 4-morpholineethanesulfonic acid; MD, molecular dynamics; r.m.s., root mean square.

environment. To the best of our knowledge, this is the first mutagenesis study of any Cyt reported up to now. The thermodynamic parameters of PSI reduction by Cyt mutants are also analyzed in a comparative way with a number of mutants of Pc modified in the east face.

EXPERIMENTAL PROCEDURES

DNA Techniques—The *pet*J gene coding for Cyt was cloned in pBluescript II (SK^+) (Stratagene) as described previously (11), thereafter being used as a template for the site-directed mutagenesis protocol. The mutant genes were constructed using the polymerase chain reaction in two steps (12). Cloning and sequencing of the modified *pet*J genes were carried out as reported previously (8) for Pc mutagenesis. Cloning and sequencing of the modified *pet*E genes encoding Pc have already been published (8). The numbering of residues of *Synechocystis* Cyt herein used is that corresponding to the heme protein from *Monoraphidium braunii* (2).

Recombinant Proteins and PSI Particles—The procedures for production and purification of mutant metalloproteins (both Cyt and Pc) were those previously described (8, 11) except that the recombinant Cyt was produced in *Escherichia coli* MC1061 cells (rather than in DH5α cells); the final yield of Cyt was 5–10-fold higher in the MC1061 strain. PSI particles were purified by β-dodecyl maltoside solubilization as described previously (7).

Redox Titrations—Redox titrations of WT Cyt and its mutants were performed in a dual wavelength spectrophotometer as described previously (8) for Pc, except that differential absorbance changes were monitored at 552−570 nm. Errors in experimental determinations were less than 5 mV.

Laser Flash Absorption Spectroscopy—Kinetics of flash-induced absorbance changes in PSI were followed at 820 nm as described previously (9). The standard reaction mixture and experimental conditions were as described previously (8), the buffer being 20 mM Tricine/KOH, pH 7.5; for experiments at pH 5.5, the buffer used was 20 mM MES/NaOH. In all cases, the standard reaction mixture contained 10 mM $MgCl_2$, which was omitted in experiments for the analysis of the ionic strength effect. For the thermodynamic analyses, experiments were run at varying temperatures (10). Data collection, as well as kinetic and thermodynamic analyses were as described previously (9, 10). Apparent thermodynamic parameters were estimated as in Díaz *et al.* (13). Electrostatic potential energies were obtained by fitting the calculated apparent activation energies to the Watkins equation (14). The errors in estimated values for the observed pseudo first-order rate constant (k_{obs}) were less than 10%.

Computer Simulations—The structures of WT Cyt and Pc, as well as that of mutants obtained by specific changes of residues were modeled using the SYBYL program (Tripos Inc.) in a SGI RC10000 workstation. The structure of WT Cyt from *Synechocystis* was modeled using the three-dimensional crystal structure of Cyt from the green alga *M. braunii* (2) as a template. The original PDB file was modified to fit the *Synechocystis* Cyt sequence with the BIOPOLYMER module of SYBYL. The resulting file was first submitted to energy minimization *in vacuo* up to an RMS energy gradient of 0.41 kJ mol^{-1} $Å^{-1}$, using the SANDER module of AMBER 4.1 (15), and then solvated with TIP3T water molecules using the BLOB option of the EDIT module. Solvent was energy minimized and submitted to a 9-ps molecular dynamics (MD) calculation. The whole system was again energy minimized and submitted to a 750-ps MD run at 300 K, from which the last 200 ps of trajectory were extracted and analyzed with CARNAL. The resulting structure (2.4 Å of RMSD from original) was again submitted to energy minimization. The quality of the structure was tested using the PROCHECK program (16). Force field parameters for the heme moiety were those included in the AMBER package (17). Models of the modified proteins were obtained by changing the residues with the BIOPOLYMER module of SYBYL and further energy minimization *in vacuo*. Surface electrostatic potentials were estimated by using the algorithm of Nicholls and Honig (18), as indicated in the MOLMOL program (19).

The structure of WT Pc from *Synechocystis* was modeled using the three-dimensional crystal structure of the triple mutant A42D/D47P/A63L (20). The structure was first submitted to restrained energy minimization, for which the cut-off radius was 6 Å for the full simulation region around the modified residue and 12 Å for the buffer region. Minimizations were performed first by the steepest descent method and second by conjugated gradient minimization until an RMS energy gradient of 0.12 kJ mol^{-1} $Å^{-1}$ was reached. TRIPOS force field parameters (21) were used. Bond lengths and dihedral angles were restrained for the copper site. A distance-dependent dielectric constant was used to simulate solvation. Surface electrostatic potentials were likewise calculated by using the algorithm of Nicholls and Honig (18), as indicated in the MOLMOL program (19).

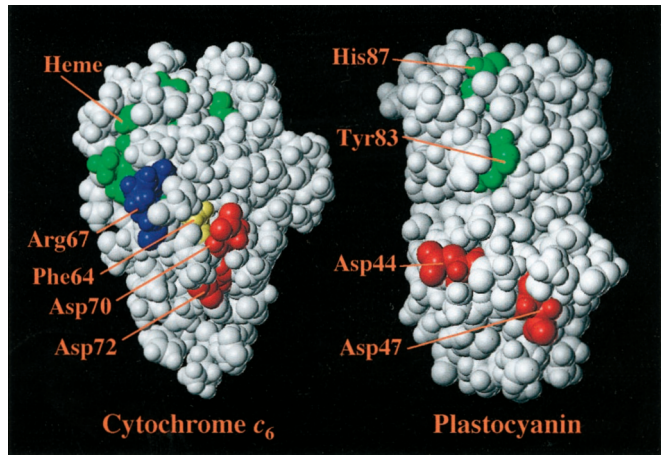

FIG. 1. **Space-filling representation of the modeled structures of cytochrome c_6 (*left*) and plastocyanin (*right*) showing the location of residues modified by site-directed mutagenesis.** The two molecules are depicted in a similar orientation, with their respective "east" faces just in front. The cytochrome molecule is oriented in such a way that the heme propionates are at the top, with the heme plane laying almost parallel to the paper. The copper protein is oriented with the so-called north hydrophobic pole at the top and the Tyr-83-surrounding area in front. The two structures were modeled as described under "Experimental Procedures."

RESULTS AND DISCUSSION

A site-directed mutagenesis study of *Synechocystis* Cyt has been performed here to investigate its structural and functional analogies with Pc. First, the three-dimesional structure of Cyt was modeled so that the mutants could properly be designed. Modeling makes evident that Cyt does possess an acidic cluster at the south-east face formed by Asp-70, Asp-72, Glu-74, Asp-75, and Asp-2. On the other hand, Tyr-83 has widely been reported to be a highly conserved residue in the east face of Pc (in the Introduction). Interestingly, Ullmann *et al.* (22) have recently proposed not only that an aromatic residue at position 64 in eukaryotic Cyt may be the counterpart of Pc Tyr-83, but also that the cation-π system between the aromatic ring of Phe-64 and the guanidinium group of Arg-67 could play a special role in electron transfer. On the basis of these data, we have mutated four specific residues in Cyt, two of them in the acidic area and the two others just outside or at the border: Asp-70 and Asp-72 were replaced by arginines; Phe-64, which is close to the heme group, was substituted by alanine; and Arg-67, which is at the edge of the east face, was changed to aspartate (Fig. 1).

Table I shows that the redox potential value of the heme group is not significantly affected by replacement of any one of the two aspartates by arginines, but it decreases in ~30 mV when Phe-64 or Arg-67 are mutated. In all cases, however, the comparative analysis of Cyt mutants by UV/visible spectroscopy reveals no changes in the heme environment (data not shown).

The capability of Cyt mutants to reduce the photooxidized chlorophyll molecule P700 in PSI particles was determined by laser flash-induced absorption spectroscopy. With the four mutants, the PSI reduction kinetic trace is monoexponential, as is it with WT Cyt, but the rate constant is drastically changed depending on the residue modified. As can be inferred from the kinetic profiles in Fig. 2 (*upper*), R67D is impaired for the reduction of PSI, but the D70R mutant is even more efficient than WT Cyt. Fig. 2 (*lower*) shows that the observed rate constant (k_{obs}) for PSI reduction with all mutants increases

TABLE I

Midpoint redox potential of wild-type (WT) and mutant cytochrome c_6 at pH 7.0 ($E_{m,7}$), and bimolecular rate constants (k_{bim} and k_∞) for the overall reaction of photosystem I reduction

Cytochrome c_6	$E_{m,7}$ (*mV*)	$k_{bim} \times 10^{-7}$ (M^{-1} s^{-1})		$k_\infty \times 10^{-7}$ (M^{-1} s^{-1})
		pH 5.5	pH 7.5	pH 7.5
WT	324	1.40	0.89	1.30
F64A	287	1.24	1.02	0.90
R67D	295	0.27	0.11	0.40
D70R	327	3.88	3.31	ND[a]
D72R	324	2.79	2.21	2.00

[a] ND, not determinable.

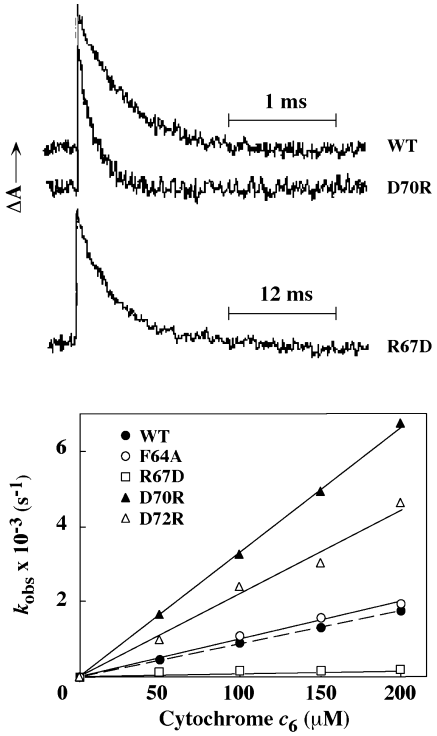

FIG. 2. **Kinetic traces showing laser flash-induced photosystem I reduction by wild-type (*WT*) and mutant species of cytochrome c_6 (*upper*) and dependence of the observed rate constant (k_{obs}) upon heme protein concentration (*lower*).** The kinetic traces were recorded at pH 7.5 with cytochrome c_6 at 200 μM final concentration.

linearly with increasing donor protein concentration up to 200 μM. As is the case not only with WT Cyt but also with WT Pc (7), such a linear dependence is interpreted by assuming that there is no formation of any kinetically detectable (or long-lived) intermediate complex between the metalloprotein and PSI. The reaction mechanism should thus involve a simple oriented collision of Cyt molecules with the membrane-anchored PSI complex. The experiments in Fig. 2 were run at pH 7.5, but similar data were obtained at pH 5.5 (not shown).

The bimolecular rate constant (k_{bim}) for the overall reaction can be obtained from the linear plots in Fig. 2. The resulting values are presented in Table I, both at pH 5.5 and 7.5. As can be seen, the mutant F64A behaves like the WT molecule, but the modification of charges in other mutants alters their rate constants: D70R and D72R yield values for k_{bim} that are 2- or 3-fold higher than those with WT Cyt, whereas the k_{bim} values with R67D are 5–8-fold lower than those with the WT protein. These findings indicate that electrostatic repulsions between residues 70 and 72 and their counterparts in PSI are hindering the interaction of the WT Cyt and that Arg-67 plays a critical role in the interaction with PSI (see below).

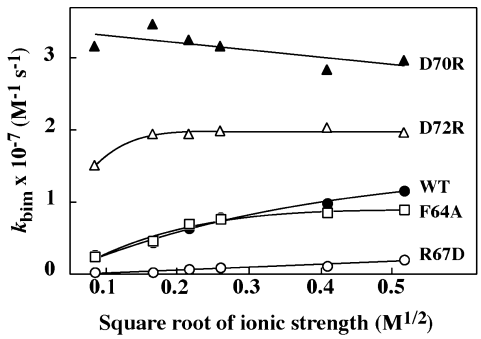

FIG. 3. **Effect of ionic strength on the second-order rate constant (k_{bim}) for the overall reaction of photosystem I reduction by wild-type (*WT*) and mutant species of cytochrome c_6.** The ionic strength was adjusted at the desired values by adding small amounts of a concentrated NaCl solution. *Solid lines* state for the fitting of experimental data (except those with D70R) to the Watkins equation (see "Results and Discussion" for further details).

TABLE II

Apparent activation parameters and changes in electrostatic energy (ΔV_{el}) for photosystem I reduction by wild-type (WT) and mutant cytochrome c_6 and plastocyanin

In all cases, the Eyring plots yielded linear regression coefficients higher than 0.99. $\Delta G^{\neq}$ was calculated at 298 K. Errors in the determination of the $\Delta G^{\neq}$ values were in the order of 0.25 kJ mol^{-1}. The values for ΔV_{el} were obtained from the experimental data in Fig. 4.

Metalloprotein	$\Delta H^{\neq}$ (kJ mol^{-1})	$\Delta S^{\neq}$ (J mol^{-1} K^{-1})	$\Delta G^{\neq}$ (kJ mol^{-1})	ΔV_{el} (kJ mol^{-1})
Cytochrome c_6				
WT	41.8	28.2	33.3	0
F64A	42.0	30.8	32.8	≈0
R67D	47.3	30.4	38.2	ND
D70R	42.5	42.1	30.0	8.5
D72R	39.0	26.6	31.1	6.8
Plastocyanin				
WT	48.2	49.9	33.4	0
D44A	44.0	36.6	33.1	2.8
D44K	44.5	42.6	31.8	13.5
D47A	47.6	50.5	32.6	1.7
D47R	44.2	36.6	33.3	8.7
D44A/D47A	45.3	44.5	32.1	10.1
D44R/D47R	35.4	17.2	30.2	23.7

[a] ND, not determinable.

Taking into account the electrostatic nature of the reaction between Cyt and PSI, the effect of ionic strength on the second-order rate constant was analyzed. As can be seen in Fig. 3, k_{bim} with WT Cyt increases with increasing NaCl concentration up to reach a maximum value at high ionic strength, indicative of repulsive interactions between the heme protein and PSI (9). The F64A mutant shows an ionic strength dependence similar to WT Cyt, as would be expected for a mutation that does not involve any charged residue. The mutant R67D, in its turn, is much less efficient in transferring electrons to PSI. Replacement of aspartate by arginine at positions 70 and 72 renders the mutant proteins slightly ionic strength-dependent, but such a substitution in position 70 makes the Cyt molecule exhibit an ionic strength dependence that is opposite that of WT Cyt.

By applying the formalism developed by Watkins (14), the bimolecular rate constant extrapolated to infinite ionic strength, that is the diffusion-limited rate constant (k_∞), can be calculated, a parameter that provides information on the intrinsic reactivity of redox partners in the absence of electrostatic interactions. The k_∞ values in Table I indicate that F64A is the only mutant that approaches WT Cyt, thereby suggesting that the other mutations involve changes that are not only electrostatic in nature. The small salt dependence of k_{bim} for D70R impeded an accurate estimation of k_∞, and the slow

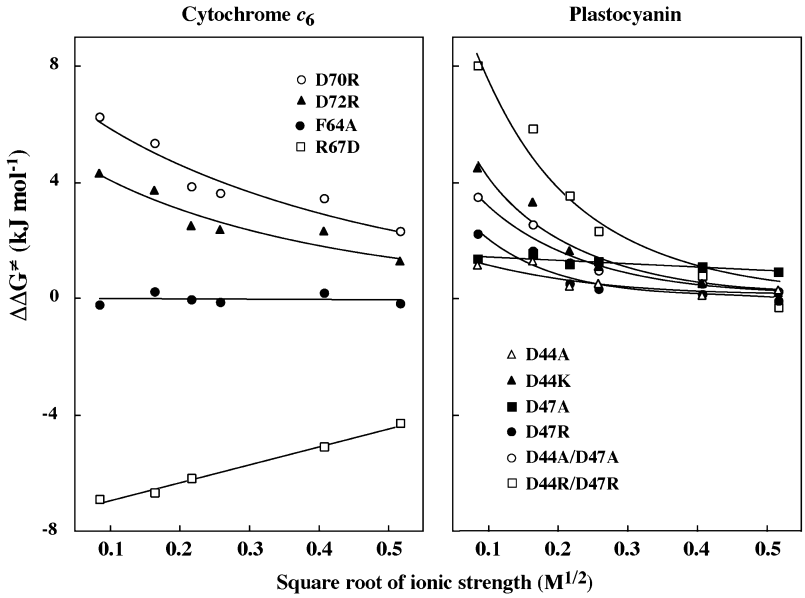

FIG. 4. **Ionic strength dependence of the changes in the apparent activation free energy ($\Delta\Delta G^{\neq}$) for photosystem I reduction by mutants of cytochrome c_6 (*left*) and plastocyanin (*right*).** The values for $\Delta\Delta G^{\neq}$ were obtained by subtracting those for $\Delta G^{\neq}$ with each mutant from $\Delta G^{\neq}$ with the WT metalloprotein. *Solid lines* indicate fitting of experimental data to Equation 2 (see "Results and Discussion" for further details).

kinetics of the R67D mutant did not allow us to get a precise value for k_{∞}.

A thermodynamic analysis was also performed to get further insights into the reaction mechanism of PSI reduction by WT and mutant Cyt. In all cases, the temperature dependence of the observed rate constant yields linear Eyring plots with no breakpoints, from which the values for the apparent activation enthalpy ($\Delta H^{\neq}$), entropy ($\Delta S^{\neq}$), and free energy ($\Delta G^{\neq}$) for the overall reaction can be calculated. As can be seen in Table II, the most drastic difference in the activation parameters is observed with R67D: its free energy value at pH 7.5 is ~5 kJ mol^{-1} higher than that of WT Cyt, as expected from its rather inefficient interaction with PSI. Such an increase in free energy is mainly because of the change in enthalpy (but not in entropy) of the system, thereby indicating that the mutation is altering just the electrostatic interactions between reaction partners. Noteworthy also is the increase in the entropic term (~14 J mol^{-1} K^{-1}) with the D70R mutant.

As reported previously (23), the bulk electrostatic effect of substitutions of charged residues can be roughly approximated by assuming that the change in the activation free energy of the overall reaction with mutants as compared with that with the WT protein ($\Delta\Delta G^{\neq}$) is directly proportional to the net charge difference between WT and mutant metalloproteins (Δq). Thus, the real effect of the mutations can be estimated by using the Watkins equation (14),

$$\ln k_{obs} = \ln k_{\infty} - V_{ii} \cdot X_k \qquad \text{(Eq. 1)}$$

where V_{ii} is the net electrostatic potential for the interaction, which depends on the electrostatic charges of the reaction partners; X_k is the Debye-Hückel term that accounts for the effect of charge screening as a function of ionic strength; and k_{∞} is the diffusion-limited kinetic rate constant. We can thus write that,

$$\Delta\Delta G^{\neq} = \Delta V_{el} \cdot X_k \qquad \text{(Eq. 2)}$$

where $\Delta V_{el}(\Delta V_{el} = \Delta V_{ii} \cdot \mathrm{RT})$ stands for the difference in electrostatic energy between the WT and mutant proteins. From Equation 2, the difference between the apparent activation free energies for WT and mutant proteins must be proportional to X_k.

As expected, the experimental data in Fig. 4 (*left*) indicate that $\Delta\Delta G^{\neq}$ changes with ionic strength according to Equation 2, but such an energetic term does not approach 0 at high ionic strength with some Cyt mutants. This finding suggests that k_{∞} is being affected not just by purely electrostatic changes, in good agreement with the entropy-dependent change in $\Delta G^{\neq}$ observed with D70R (see above). To account for these discrepancies, a new term should be added to Equation 2,

$$\Delta\Delta G^{\neq} = \Delta V_{el} \cdot X_k + \mathrm{RT} \ln (k_{\infty}^{WT}/k_{\infty}^{mutant}) \qquad \text{(Eq. 3)}$$

in which the relative value of k_{∞} with mutants as compared with that with the WT protein is considered. The experimental data in Fig. 4 were thus fitted to Equation 3, from which the values for ΔV_{el} with the mutants D70R and D72R were estimated (Table II). F64A exhibits a 0 value for ΔV_{el}, as expected from its kinetic behavior close to the WT Cyt; with D67R, in turn, it was not possible to determine a value for ΔV_{el} as $\Delta\Delta G^{\neq}$ depends linearly on ionic strength (see Fig. 4).

A comparative thermodynamic study was carried out with a set of mutants of *Synechocystis* Pc, which was modified by replacing specific residues in the east patch. We have previously reported that the values of k_{obs} for PSI reduction, at the ionic strengths used throughout this work, depend linearly on Pc concentration with all mutants of *Synechocystis* Pc—even with the double mutant D44R/D47R, which reaches a saturation plateau at lower ionic strength that suggests the formation of an electrostatic transient complex with PSI (8).

The activation parameters of the electron transfer reaction between modified Pc and PSI have thus been analyzed here in a similar way than those with Cyt and its mutants. Fig. 4 (*right*) shows the effect of ionic strength on $\Delta\Delta G^{\neq}$ for the mutants of *Synechocystis* Pc. The experimental data indicates that $\Delta\Delta G^{\neq}$ changes with ionic strength according to Equation 2, thereby indicating that the changes in this area alter the rate constants as a consequence of the changes in the bulk electrostatics of the interaction. In principle, the relative effect of amino acid substitutions can directly be related to the net change in charge Δq. Actually, the values for $\Delta\Delta G^{\neq}$ at low ionic strength with D44R/D47R ($\Delta q = 4$) are approximately 2-fold higher than those with D44K and D44A/D47A ($\Delta q = 2$).

Table II shows the apparent activation parameters, as calculated from the Eyring plots under standard conditions, for the reduction of PSI by WT and mutant Pc. It also shows the values for ΔV_{el} obtained by fitting the experimental data in Fig. 4 to Equation 2. As expected, the differences in $\Delta G^{\neq}$ between WT and any mutant Pc are proportional to ΔV_{el}, the D44R/

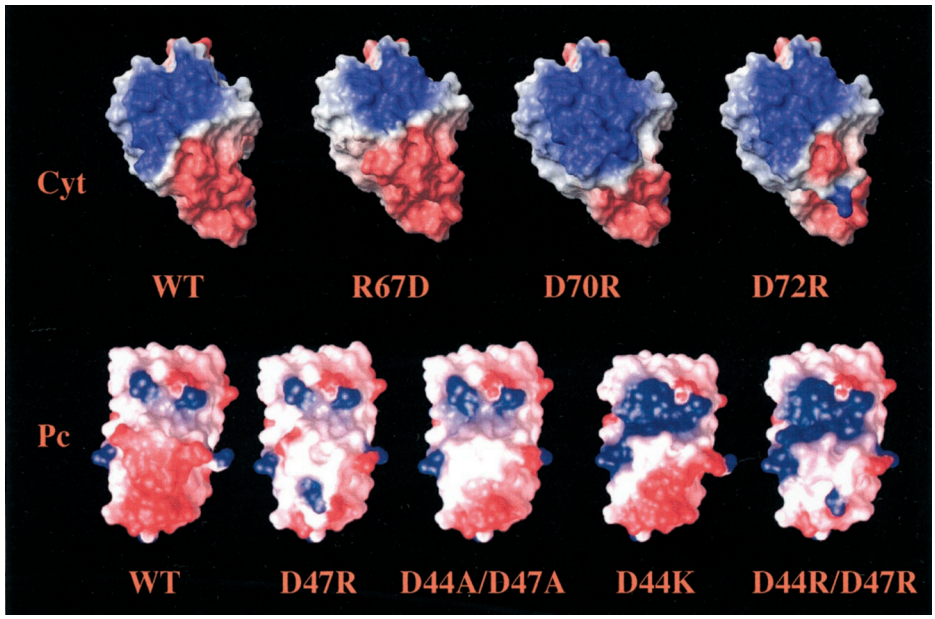

FIG. 5. **Electrostatic potential distribution on the surface of wild-type (*WT*) and mutants of cytochrome c_6 (*upper*) and plastocyanin (*lower*).** Surface electrostatic potential was calculated as indicated under "Experimental Procedures." Simulations were performed assuming an ionic strength of 40 mM at pH 7. Negative and positive potential regions are depicted in *red* and *blue*, respectively. The relative orientation of the heme and copper proteins is as described in the legend to Fig. 1.

D47R mutant in fact showing the largest value for ΔV_{el} as well as the smallest one for $\Delta G^{\neq}$.

The ΔV_{el} values change from one to another Pc mutant, even when there is no difference in Δq. The mutations are thus affecting in a different manner the electrostatic interaction energy, with the relative effect of mutation on ΔV_{el} depending not only on Δq but also on the specific location of the modified residue in the protein surface. Actually, when mutations involving the same net charge difference are performed in residues Asp-44 and/or Asp-47, the ΔV_{el} value with mutants at position 44 is always larger than that with mutants at position 47 (see Table II). Such a finding indicates that the changes in reactivity mainly depend on the net charge difference Δq, but it is specifically the local negative potential in the proximity of residue 44 that determines the repulsion between reaction partners.

A computer simulation of the distribution of surface electrostatic potential in the mutants of Cyt was compared with that in the mutants of Pc (Fig. 5). Asp-70 in Cyt and Asp-44 in Pc are located near the interphase between the acidic patch and a positively charged region, whereas Asp-72 in Cyt and Asp-47 in Pc are just located in the middle of the acidic patch (see also Fig. 1). Hence, the positive charge introduced upon mutation of any one of the latter residues to arginine is screened by the surrounding negative ones, whereas mutations at the interphase between the two regions result in a rather large modification of the electrostatic potential. In Cyt, the replacement of Asp-70 by arginine induces a spread of the positively charged region, whereas the mutation D72R has a reduced effect on the electrostatic potential. In Pc, the single mutation in D44K as well as the double replacement in D44A/D47A induce a significant increase in the positively charged area closer to the hydrophobic north pole. In addition, the double substitution in D44R/D47R induces an inversion of the electrostatic potential at the eastern patch of Pc, so enabling a large, long range electrostatic attraction toward the reaction center.

In the MD model of *Synechocystis* Cyt, Phe-64 points toward inside the protein, with the aromatic ring dwelling close to the heme group in such a way that a small reorganization of the Arg-67 side chain could bring the guanidinium group toward the aromatic ring of Phe-64. However, the much lower reactivity of the Cyt R67D mutant cannot be explained on Ullmann's hypothesis (see above). In fact, the replacement of Phe-64 by alanine yields a mutant with the same kinetic efficiency as the WT molecule, thus indicating not only that the aromatic residue is not crucial for the interaction of Cyt with PSI but also that the cation-π interaction is not necessary for electron transfer to PSI. We should however bear in mind that Cyt has to interact also with the cytochrome b_6f complex, for which the aromatic residue would be required (22, 24). In a similar way, Tyr-83 in Pc has been reported to be involved in the interaction with cytochrome *f* but not with PSI (4, 25, 26). In this context, Sebban-Kreuzer *et al.* (27) have shown that a tyrosine residue at position 64 is essential for electron transfer between *Desulfovibrio vulgaris* cytochrome c_{553} and its formate dehydrogenase. Whether or not Phe-64 plays any role in the redox interaction with cytochrome *f*, its vicinity both to the heme group and to Arg-67 would explain why the mutation in Phe-64 leads to changes in the redox potential value (see Table I).

We conclude that Cyt possesses a negatively charged cluster that is isofunctional with the "south-east" patch of Pc. Despite the large positively charged region on the north-east face of WT Cyt, such an acidic patch should be responsible for the repulsive interactions with PSI at low ionic strength.

Acknowledgment—The authors thank Fernando P. Molina-Heredia for help in expressing the recombinant heme proteins.

REFERENCES

1. Navarro, J. A., Hervás, M., and De la Rosa, M. A. (1997) *J. Biol. Inorg. Chem.* **2,** 11–22
2. Frazão, C., Soares, C. M., Carrondo, M. A., Pohl, E., Dauter, Z., Wilson, K. S., Hervás, M., Navarro, J. A., De la Rosa, M. A., and Sheldrick, G. (1995) *Structure* (*Lond.*) **3,** 1159–1169
3. Nordling, M., Sigfridsson, K., Young, S., Lundberg, L. G., and Hansson, Ö. (1991) *FEBS Lett.* **291,** 327–330
4. Haehnel, W., Jansen, T., Gause, K., Klösgen, R. B., Stahl, B., Michl, D., Huvermann, B., Karas, M., and Herrmann, R. G. (1994) *EMBO J.* **13,** 1028–1038
5. Hippler, M., Reichert, J., Sutter, M., Zak, E., Altschmied, L., Schröer, U., Herrmann, R. G., and Haehnel, W. (1996) *EMBO J.* **15,** 6374–6384
6. Sigfridsson, K., Young, S., and Hansson, Ö. (1996) *Biochemistry* **35,** 1249–1257
7. Hervás, M., Ortega, J. M., Navarro, J. A., De la Rosa, M. A., and Bottin H. (1994) *Biochim. Biophys. Acta* **1184,** 235–241
8. De la Cerda, B., Navarro, J. A., Hervás, M., and De la Rosa, M. A. (1997) *Biochemistry* **36,** 10125–10130
9. Hervás, M., Navarro, J. A., Díaz, A., Bottin, H., and De la Rosa, M. A. (1995) *Biochemistry* **34,** 11321–11326
10. Hervás, M., Navarro, J. A., Díaz, A., and De la Rosa, M. A. (1996) *Biochemistry* **35,** 2693–2698
11. Hervás, M., Navarro, F., Navarro, J. A., Chávez, S., Díaz, A., Florencio, F. J., and De la Rosa, M. A. (1993) *FEBS Lett.* **319,** 257–260
12. Giebel, L. B., and Spritz R. A. (1990) *Nucleic Acids Res.* **18,** 4947

13. Díaz, A., Hervás, M., Navarro, J. A., De la Rosa, M. A., and Tollin, G. (1994) *Eur. J. Biochem.* **222,** 1001–1007
14. Watkins, J. A., Cusanovich, M. A., Meyer, T. E., and Tollin, G. (1994) *Protein Sci.* **3,** 2104–2114
15. Pearlman, D. A., Case, D. A., Cadwell, G. C., Siebel, G. L., Singh, U. C., Weiner, P., and Kollman, P. A. (1995) AMBER 4.1. University of California, San Francisco, CA
16. Laskowski, R. A., MacArthur, M. W., Moss, D. S., and Thornton, J. M. (1993) *J. Appl. Crystallogr.* **26,** 283–291
17. Giammona, D. A. (1984) Ph. D. Thesis. University of California, Davis, CA
18. Nicholls, A., and Honig, B. (1991) *J. Comput. Chem.* **12,** 435–445
19. Koradi, R., Billeter, M., and Wuthrich, K. (1996) *J. Mol. Graph.* **14,** 51–55
20. Romero, A., De la Cerda, B., Varela, P. F., Navarro, J. A., Hervás, M., and De la Rosa, M. A. (1998) *J. Mol. Biol.* **275,** 327–336
21. Clark, M., Cramer, R. D., and Van Opdenbosh, N. (1989) *J. Comput. Chem.* **10,** 982–1012
22. Ullmann, G. M., Hauswald, M., Jensen, A., Kostic, N. M., and Knapp, E.-W. (1997) *Biochemistry* **36,** 16187–16196
23. Kannt, A., Young, S., and Bendall, D. S. (1996) *Biochim. Biophys. Acta* **1277,** 115–126
24. Ullmann, G. M., Knapp, E.-W., and Kostic, N. M. (1997) *J. Am. Chem. Soc.* **119,** 42–52
25. Modi, S., Nordling, M., Lundberg, L. G., Hannson, Ö., and Bendall, D. S. (1992) *Biochim. Biophys. Acta* **1102,** 85–90
26. Modi, S., He, S., Gray, J. C., and Bendall, D. S. (1992) *Biochim. Biophys. Acta* **1101,** 64–68
27. Sebban-Kreuzer, C., Blackledge, M., Dolla, A., Marion, D., and Guerlesquin, F. (1998) *Biochemistry* **37,** 8331–8340